

Photoemission from Polycyclic Aromatic Crystals in the Vacuum Ultraviolet Region. III. Aromatic Crystals and Charge-transfer Complexes

Tomohiko HIROOKA, Masakatsu KOCHI, Jun-ichi AIHARA,
Hiroo INOKUCHI and Yoshiya HARADA

The Institute for Solid State Physics, The University of Tokyo, Roppongi, Tokyo

(Received September 25, 1968)

The photoemission from various types of charge-transfer complexes, quinolinium-tetracyanoquinodimethane $Q(TCNQ)_2$ (I), dibenzophenothiazine (DBP)-dicyanodichloro-*p*-benzoquinone (DDQ)[(DBP)(DDQ)(II)] and (DBP)₂(DDQ)(III)], trinitrobenzene (TNB)-coronene (IV), and TNB-perylene (V), and also large polycyclic aromatic hydrocarbons, violanthrene A (VI), violanthrene B (VII), coronene (VIII), pyranthrene (IX), and pyranthrone (X), was observed in the vacuum ultraviolet region. The experimental equation $Y \propto (E - E^*)^3$, where Y is the quantum yield of photoemission; E , the incident photon energy, and E^* , the threshold energy, was used to determine the ionization potential. The E^* -values, as estimated from the experimental equation, were I=4.85 eV, II 4.99, III 4.75, IV 5.62, V 5.52, VI 5.06, VII 5.13, VIII 5.58, IX 5.04, and X=5.71 eV. A band structure scheme for these organic semiconductors was introduced to analyse the emission mechanism.

In 1935, the spectral dependence of the photoemission from the naphthalene and anthracene complexes with alkali metals was observed by Suhrmann.¹⁾ In 1963, Inokuchi and Harada²⁾ reported their findings on the violanthrene A complex with cesium; further, Ogino *et al.*,³⁾ measured the dependence of the pyrene derivatives complexes with cesium. However, the photoemission from the charge-transfer complexes, the components of which are organic substances, were not observed until recently because the wavelength region of the photoemission from them is in the vacuum ultraviolet region where measurement is difficult. On the other hand, we have already reported our findings on the current-voltage characteristics and the spectral distributions of the photoemission from polycyclic aromatic hydrocarbons.^{4,5)} Recently Batley and Lyons⁶⁾ reported on the photoemission from the 1,6-diaminopyrene and the tetramethyl-*p*-phenylenediamine-complexes with various organic acceptors.

In the above previous works, two methods of determining the ionization potential of solid have been used. One was the method of obtaining the ionization potential from the threshold energy of the spectral response of the photoemission. Lyons and Morris⁷⁾ determined the threshold as the lowest detectable current. However, in this method, it is necessary for the photoemission yield to rise up abruptly at the threshold energy; this condition is not necessarily satisfied in all compounds. For instance, the bulk ionization potentials determined by Kearns and Calvin⁸⁾ by this method were too small in comparison with the values obtained by the other methods.

The second method was that of the retarding potential. Terenin and Vilesov⁹⁾ obtained the ionization potential by measuring a current-stopping potential and also a current-saturation potential. When the sample has a semiconductive character, however, it is very difficult to determine the current-stopping potential because the current becomes an asymptotic curve to the voltage axis in its neighbourhood.¹⁰⁾

1) R. Suhrmann and D. Dempster, *Z. Phys.*, **94**, 742 (1935); *ibid.*, **111**, 18 (1937).

2) H. Inokuchi and Y. Harada, *Nature*, **198**, 477 (1963).

3) K. Ogino, S. Iwashima, H. Inokuchi and Y. Harada, *This Bulletin*, **38**, 473 (1965).

4) Y. Harada and H. Inokuchi, *This Bulletin*, **39**, 1443 (1966).

5) M. Kochi, Y. Harada and H. Inokuchi, *ibid.*, **40**, 531 (1967).

6) M. Batley and L. E. Lyons, *Mol. Cryst.*, **3**, 357 (1968).

7) L. E. Lyons and G. C. Morris, *J. Chem. Soc.*, **1960**, 5192.

8) D. R. Kearns and M. Calvin, *J. Chem. Phys.*, **34**, 2026 (1961).

9) A. Terenin and F. Vilesov, "Advances in Photochemistry," Vol. II, Interscience Publishers, New York (1964), p. 407.

10) See the schematic diagram of the voltage-current characteristics for an intrinsic semiconductor given by L. Apker, E. Taft and J. Dickey, *Phys. Rev.*, **74**, 1462 (1948).

This paper will give the results of the photoemission from various types of charge-transfer complexes and large polycyclic aromatic hydrocarbons. Because the voltage-current characteristic of the charge-transfer complexes used in this work is intrinsic semiconductor-like and because the photoemission yield does not rise up abruptly at the threshold energy, their ionization potentials can not be determined by the above two methods. Therefore, an experimental equation will be employed in this study to determine the ionization potential.

Experimental

Materials. The materials used in the present study are shown in Figs. 1 and 2. Figure 1 shows the structural formula of the condensed aromatic hydrocarbons—violanthrene A, violanthrene B, coronene, pyranthrene and pyranthrone. Figure 2 illustrates those of the charge-transfer complexes—quinolinium-tetracyanoquinodimethane $Q(TCNQ)_2$ and dibenzophenothiazine (DBP)-dicyanodichloro-*p*-benzoquinone (DDQ); these are two different complexes with different component ratios, (DBP)(DDQ) and $(DBP)_2(DDQ)$. The other charge-transfer complexes used are trinitrobenzene (TNB)-coronene and TNB-perylene.

Sample Preparation. Except for $Q(TCNQ)_2$, the materials were deposited on a copper disc, 10 mm in diameter, by means of sublimation *in vacuo* (10^{-5} – 10^{-6} mmHg). The deposited films were several microns thick. The $Q(TCNQ)_2$ complex could not be sublimed. Therefore, as it had a high electrical conductivity in the bulk state, the complex could be used as a pressed disc stuck with silver paste onto the copper disc. The pressed sample was approximately 1 mm thick.

The formation of the complex was examined by means of the absorption spectra of the sublimed samples. We observed that (DBP)(DDQ) and $(DBP)_2(DDQ)$ have different absorption spectra, both of which possess a characteristic charge-transfer band near 7400Å.

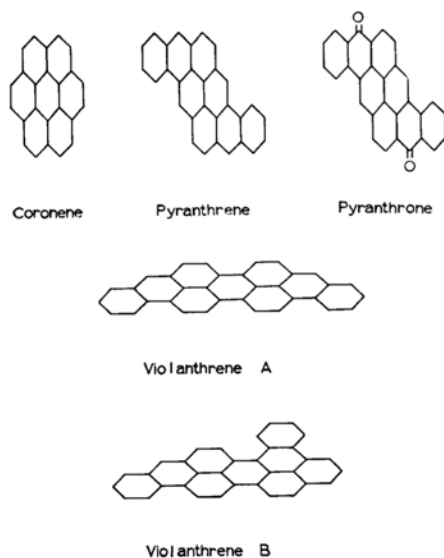


Fig. 1. The structural formulas of the condensed aromatic hydrocarbons.

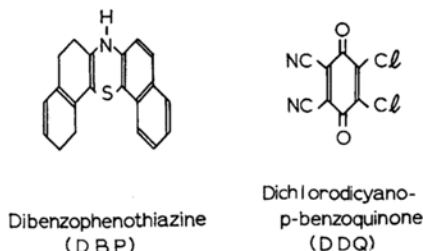
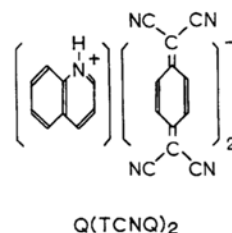


Fig. 2. The structural formulas of the charge-transfer complexes.

To observe the photoemission, a Seya-Namioka-type vacuum ultraviolet monochromator was used. The details of the apparatus have been reported previously.⁴⁾ The collector of the photoemissive cell, a glass sphere, was about 13 cm in diameter. On the inside it was coated with a conducting layer of colloidal graphite, Aquadag. The sample was placed in the centre of the cell. In order to obtain enough intensity, the slit was made 1 mm wide at the cost of resolving power. The photoemission current was amplified and observed by a Cary 31 vibrating-reed electrometer.

The spectral dependence of the photoemission yield was measured under an applied potential of 10 V, enough to gather all of the emitting electrons, and at intervals of 20Å. The saturation of the photoemission current for $Q(TCNQ)_2$ against an applied potential was very slow, but the current observed around 50V was saturated enough for us to estimate the photoemission yield.

The current-voltage characteristics were observed by a spherical retarding method, and the photoemission current was recorded as a function of the applied voltage with a Yokogawa X-Y recorder, PRO-12. The current saturation potential, V_s , was determined by averaging the values observed at the incident wavelength of 1600Å, 1400Å, or 1200Å. In the present study, a highly accurate saturation point was obtained because the photocell used had a good spherical geometry. This observation was carried out to a precision of less than 0.03 eV.

Results and Discussion

Figure 3 shows the photoelectric yield curves of violanthrene A and violanthrene B as functions of the incident photon energy. Figure 4 shows those of pyranthrene and pyranthrone. The threshold energy, E_{th} , can be determined by extrapolation to a quantum yield of 10^{-7} electrons per incident quantum. However, as is shown in Figs. 3 and 4,

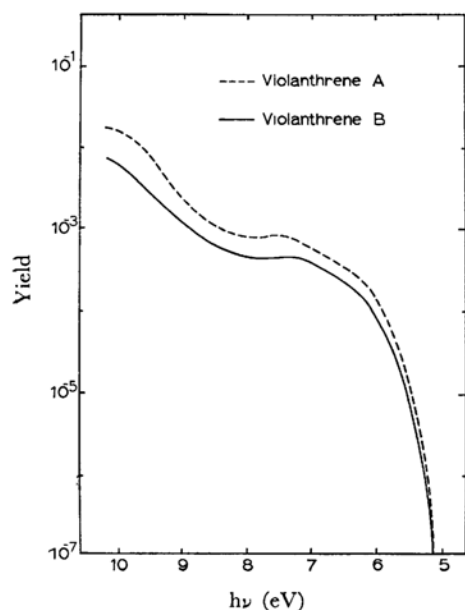


Fig. 3. The photoelectric yield curves of violanthrene A and violanthrene B.

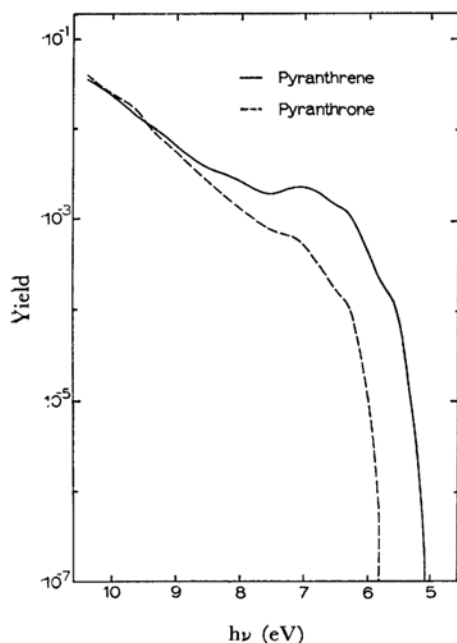


Fig. 4. The photoelectric yield curves of pyranthrene and pyranthrone.

the shapes of the rising photoemission yield curves from the threshold point are different in various compounds. For instance, violanthrene A and violanthrene B are found to have the same threshold energy by the extrapolation method described above, but the shapes of the rising photoemission yield curves are clearly different.

The spectral response patterns of the yield are very different in the two types of charge-transfer complexes used in the present study. One of them is a weak charge-transfer complex, while the other is a strong charge-transfer complex. Figure 5 shows the spectra dependence of the photoemission yield of two weak charge-transfer complexes (CT-complexes), TNB-coronene and TNB-perylene.

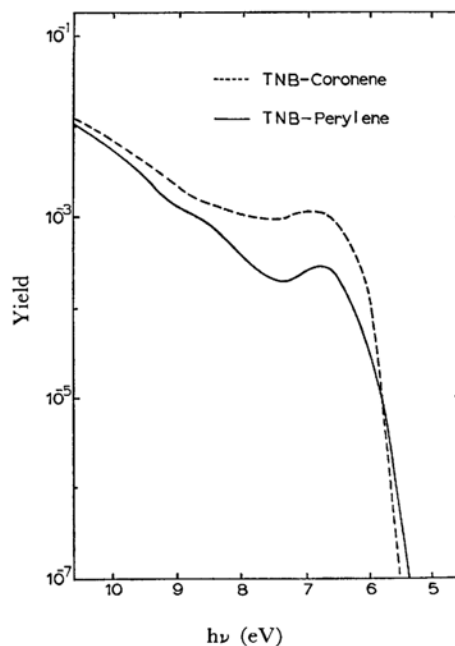


Fig. 5. The photoelectric yield curves of the weak charge-transfer complexes, TNB-coronene and TNB-perylene.

In the case of weak CT-complexes, the photoemission yield curves are almost the same as that of the donor component; for instance, the yield curve of (TNB)-coronene has a peak at about 6.7 eV corresponding to that of coronene.*¹ The ionization potential of the acceptor (TNB) is estimated to be higher than that of the donor (coronene), therefore, the ionization potential of the complex can be determined by means of the threshold energy of only the donor (coronene). Figures 6 and 7 show the spectral responses of the yields of the strong charge-transfer complexes—Q (TCNQ)₂, (DBP)-(DDQ), and (DBP)₂(DDQ).

The photoemission yield curves of their separated components are shown in the same figure for comparison. In Fig. 7 the characteristic peak is observed at about 7.3 eV; this value, corresponds to

*¹ This suggests that, in weak charge-transfer complexes, the two components keep their individual characteristics, so the total photoemission from complexes is almost equal to the superposition of those of the two components.

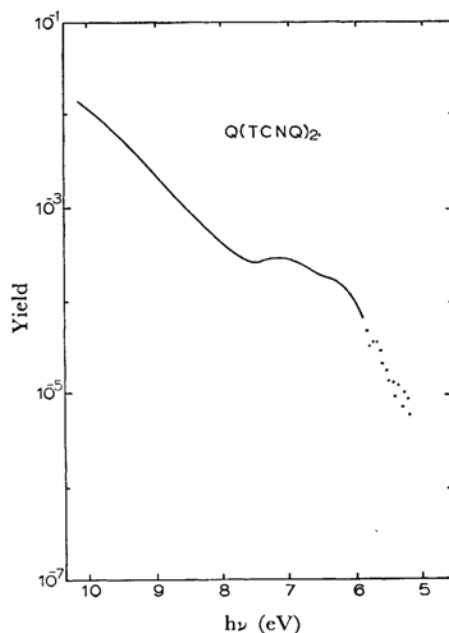


Fig. 6. The spectral response of the photoemission yield of the strong charge-transfer complex, $Q(TCNQ)_2$.

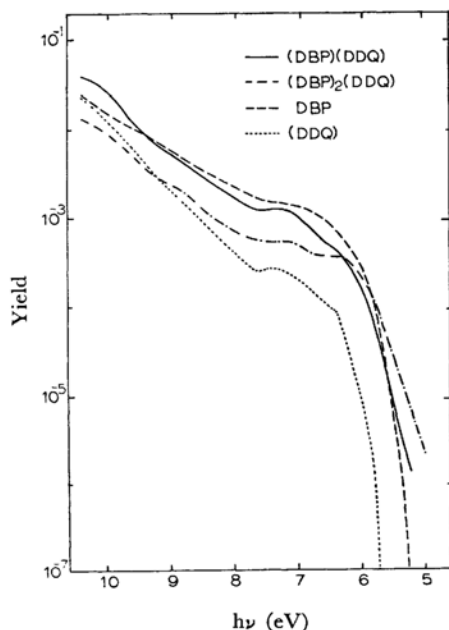


Fig. 7. The spectral response of the photoemission yield of the strong charge-transfer complexes, $(DBP)(DDQ)$, $(DBP)_2(DDQ)$ and their components.

that of the acceptor, DDQ. In $(DBP)_2(DDQ)$ a new peak is observed at about 6.4 eV.

The quantum yield near the threshold energy of the strong charge-transfer complexes decreased very slowly in comparison with the other materials;

therefore, the threshold energy could not be determined by the extrapolation method.

By analogy with the Fowler plot for metal, we assumed that the quantum yield in organic crystals near the threshold energy is subject to the conventional power law;^{*2}

$$Y \propto (E - E^*)^n \quad (1)$$

where Y is the quantum yield, E , the incident photon energy, and E^* , the threshold energy.

Figure 8 shows the spectral dependence of the photoemission yield of $(DBP)(DDQ)$ as plotted with $n=1, 2$, and 3 . This indicates that, in the lower-energy part, a cube root plot of the quantum yield becomes almost linear as a function of the incident photon energy, while in the higher-energy part the quantum yield becomes linear. The same equation, Eq. (1), was applied to the photoemission from inorganic crystals.¹²⁾ This empirical cube root law held true for all the compounds studied.

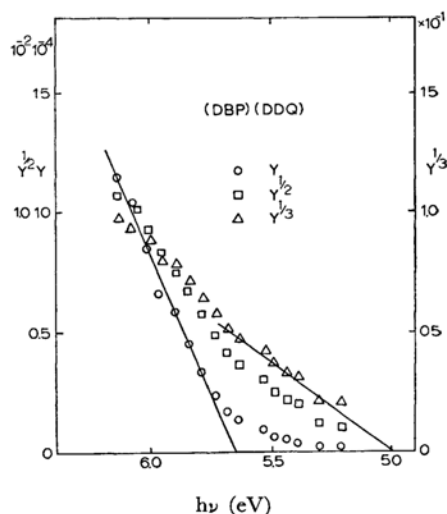


Fig. 8. The linear, square and cube root plot of the yield of $(DBP)(DDQ)$ near the threshold energy.

^{*2} In inorganic semiconductors, Kane¹¹⁾ proposed that the spectral yield obeys $Y \propto (E - E^*)^n$, in which $n=1, 3/2, 2$, and $5/2$ under various conditions near the threshold energy. Gobel and Allen¹²⁾ observed that, for an atomically-clean silicon surface, the spectral yield curve was composed of two components. One of them is the part of a linear plot of the yield which corresponds to a direct transition, while the other is the part of a cube root plot at a lower photon energy which corresponds to an indirect transition. Kane's theory was obtained assuming that the band theory can be strictly applied. However, it is doubtful whether it can be applied to organic crystals with narrow band widths.

11) E. O. Kane, *Phys. Rev.*, **127**, 131 (1962).

12) G. W. Gobel and F. G. Allen, *ibid.*, **127**, 141 (1962).

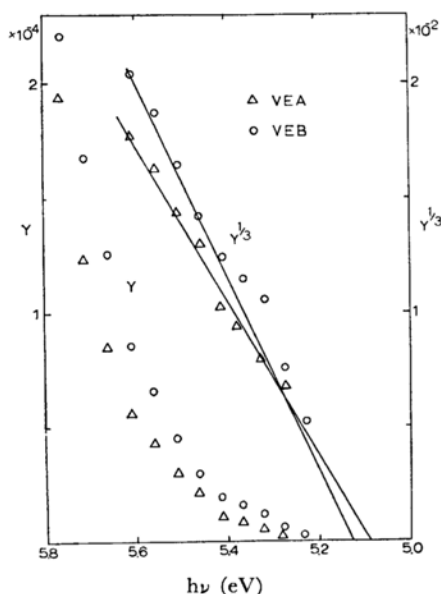


Fig. 9. The linear and cube root plot of the photoemission yield of violanthrene A and violanthrene B near the threshold energy.

Figure 9 shows the cube root plot and the linear plot of violanthrene A and violanthrene B. The difference in the photoemission yield curve near the threshold energy leads to the difference in the threshold energy, E^* .

This method can be applied to the complexes, and their threshold energy can be thus determined. For both the single component compounds and the complexes used, the cube root plot gives a straight line for the energy region of 0.3 eV—0.6 eV from the threshold energy. The E_{th} values and also the E^* values obtained by this method are given in Table 1. As this table shows, the E_{th} and E^* of single component compounds agree within the limits of 0.15 eV. Especially for the compounds which have an abrupt increase in the quantum yield

near the threshold energy, the threshold energy values obtained by the extrapolation method need not be modified.

The values of the ionization potential are 0.37 eV for (DBP)(DDQ) and 0.61 eV for (DBP)₂(DDQ) respectively, both values being smaller than that of the donor, DBP. If this difference is caused by any impurity which has a lower threshold energy, the quantum yield will not be subjected to the cube root law, because perhaps the impurity is only small in amount. Batley and Lyons⁶⁾ explained it as being due to the difference in polarization energy for the non-ionic complexes. For the ionic complexes they used the different explanation that the emission comes from the negative ion. The strong charge-transfer complexes in the present study have the properties between the weak charge-transfer complexes and the ionic complexes.

If we assume that the organic molecular crystals used as emitters are intrinsic semiconductors, and if a metal is used as the collector, the schematic diagram in Fig. 10 can be introduced. The Fermi level of the emitter coincides with that of the collector in thermal equilibrium. The potential difference between the vacuum level of a collector and the vacuum level of an emitter corresponds to the current saturation potential, V_s . The work function, ϕ , of the emitter, which corresponds to the energy difference between the vacuum level of the emitter and the Fermi level, is obtained as;

$$\phi = \phi_c - eV_s = 4.74 - eV_s \quad (2)$$

where ϕ_c is the work function of the collector. Aquadag (colloidal graphite) is used as the collector in our study. The value of ϕ_c for Aquadag is 4.74 eV.¹⁰⁾

Work functions can be determined independently by means of the contact potential difference method. Kotani and Akamatsu¹³⁾ determined the work functions of the organic crystals using this method. Table 2 shows the work functions obtained by means of these two methods. The table indicates

TABLE 1. THE IONIZATION POTENTIAL OF THE POLYCYCLIC AROMATIC COMPOUNDS AND THE CHARGE-TRANSFER COMPLEXES

Material	E_{th} (eV)	E^* (eV)
Coronene	5.59	5.58
Violanthrene A	5.20	5.06
Violanthrene B	5.20	5.13
Pyranthrene	5.05	5.04
Pyranthrone	5.83	5.71
Q(TCNQ) ₂	—	4.85
(DBP)(DDQ)	—	4.99
(DBP) ₂ (DDQ)	—	4.75
DBP	5.21	5.36
DDQ	5.68	5.64
TNB-coronene	—	5.62
TNB-perylene	—	5.52

TABLE 2. THE WORK FUNCTION (ϕ) OF THE POLYCYCLIC AROMATIC COMPOUNDS AND THE CHARGE-TRANSFER COMPLEXES

Material	ϕ	ϕ_{CPD}^*	V_s
Coronene	4.70	—	0.04
Violanthrene A	4.50	4.50	0.24
Pyranthrene	4.54	4.50	0.20
Pyranthrone	4.52	—	0.22
(DBP)(DDQ)	4.63	4.58±0.04	0.11
(DBP) ₂ (DDQ)	4.62	4.60±0.01	0.12
DDQ	4.75	—	-0.01

* The values obtained from the contact potential difference method by Kotani and Akamatsu.¹³⁾

13) M. Kotani and H. Akamatsu, private communication.

that the two work functions are in fairly good agreement.

In the case of the intrinsic semiconductor, the energy difference, δ ,^{*3} between the top of the valence band and the Fermi level is a half of the band-gap energy, $\Delta\epsilon/2$, based on the results of the temperature dependence of the semiconduction. If we use the work functions, ϕ , in Table 2, the band-gap energy, $\Delta\epsilon$, can be estimated from the following equation:

^{*3} Indicated in Fig. 10.

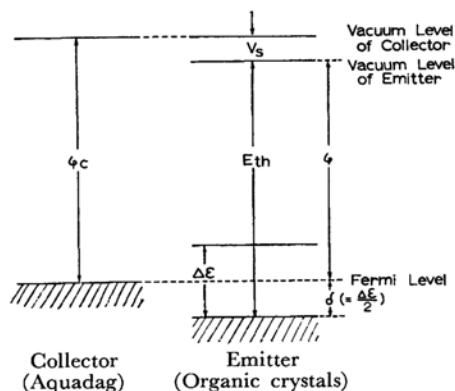


Fig. 10. The schematic diagram for the external photoelectric process of the organic molecular crystal.

^{*4} In previous works,^{4,5} E_{th} was used as a threshold value instead of E^* .

TABLE 3. THE ENERGY GAP ($\Delta\epsilon$) ESTIMATED FROM EQ. (3)

Material	$\Delta\epsilon$	$\Delta\epsilon_r^*$
Coronene	1.78	1.7 ^{a)}
Violanthrene A	1.12	0.9 ^{b)}
Pyranthrene	1.00	1.07 ^{b)}
(DBP)(DDQ)	0.72	0.54 ^{c)}
(DBP) ₂ (DDQ)	0.26	0.18 ^{c)}
DDQ	1.78	—

* Observed from the temperature dependence of the electrical conductivity.

a) H. Inokuchi, H. Kuroda and H. Akamatu, This Bulletin, **34**, 749 (1961).

b) H. Inokuchi, *ibid.*, **24**, 222 (1951).

c) Y. Matsunaga, *J. Chem. Phys.*, **42**, 1982 (1965).

$$\Delta\epsilon = 2(E^* - \phi) = 2(E^* - \phi_c + eV_s) \quad (3)^{*4}$$

In Table 3, the $\Delta\epsilon$ values obtained in this way are compared with those found from the temperature dependence of the semiconduction. The two values are in fairly good agreement in spite of the rough assumption. This result suggests that the energy level diagram used is a good assumption.

We wish to thank Professors Yoshio Matsunaga and Junji Aoki, and Mr. Satoshi Iwashima for supplying us with the organic materials.